Stochastic Analysis of Aeroradiometric Data for Characterisation of Uranium Favourbility In the Lower Proterozoic Vempalle Formation, Cuddapah Basin, Andhra Pradesh, India

A.P. DHURANDHAR
Orion Geohytech, G10 Bramhaputra Apartment Aakar Nagar, Katol Road, Nagpur, India, 440013
apdhurandhar@gmail.com

Abstract: Airborne Gamma Ray Spectrometric (AGRS) data analysis for the southern Cuddapah basin revealed many radioactive anomalies in the Proterozoic Vempalle formation. Geological and Geochemical analysis of aeroradiometric data for Komanutola and Giddankipalle blocks shows high eU, eU/eTh and eU/K ratios of phosphatic dolomite of Lower Vempalle Formation lead to define the Uranium Favourability Index (UFI). The UFI maps for Komanutola and Giddankipalle areas have indicated ESE-WNW to E-W trending linear anomalous zones for uranium mineralisation within the Vempalle phosphatic dolomite. UFI 10 to 38 corresponds to 0.01 to 0.04%eU_3O_8 values on surface outcrop samples.

Keywords: Airborne Gamma Ray Spectrometric data**,** Stochastic Analysis, Vempalle Formation, Uranium Favourability Index.

1. Introduction

The Atomic Minerals Directorate of the Department of Atomic Energy India has been carrying out Airborne Gamma-ray Spectrometric (AGRS) surveys since 1970. The foremost objective of the surveys is to target the areas of greatest possibility of finding uranium deposit. This technique has also been successfully used for environmental monitoring around nuclear power plants (Katti et al. 1997, Youssef and Elkhodary 2013) and for hydrocarbon exploration (Armstrong and Heemstra, 1973, Busby et al.1991, Sikka and Shives, 2002). AGRS is a tool for rapid large-scale geological mapping (Neuschel 1970, 71 Darnley 1970, 71 and 73 Darnley and Grasty 1971). Generally, AGRS data are interpreted in terms of bed rock geology, where the soils are developed in situ, they are similar to their underlying parent rock in thorium, uranium, and potassium contents and preserve lithological contacts (Darnley and Fleet 1968, Pitkin 1968, Schwarzer et. al., 1972, Grasty and Minty, 1995, IAEA 1991, and 2003). With this analogy, AGRS stack profile data is classified into litho-geochemical categories and are analyzed by using global geochemical continuum model (Fig.1).

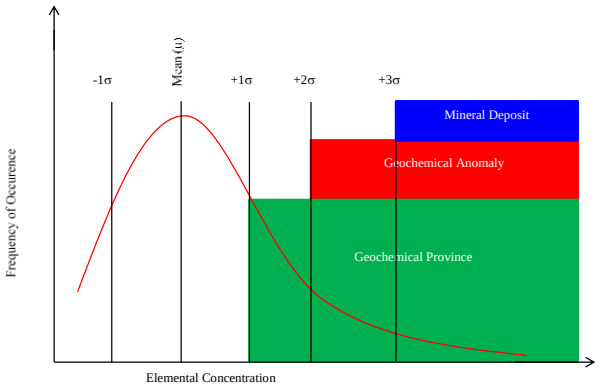

Figure 1: Geochemical Continuum

If one were to plot a histogram of the frequency of occurrence of all the sample analyses in the world for a particular element, the vast majority of the values would lie at or near the crustal abundance. A geochemically enriched province will show consistently higher mean value and a large variance than the province characterized by normal value near the crustal abundance (Saunders, 1979). Preliminary scanning of AGRS analog data for southern Cuddapah basin Andhra Pradesh revealed abnormally high uranium median value and clustering of smaller uranium enriched areas in the phosphatic dolomite of Lower Vempalle Formation. Two such anomalous areas around Komanutola and Giddankipalle were selected for detail geological and geochemical analyses (Fig. 1b and 1c).

2. Data Acquisition and Pre-Processing

AGRS data was recorded using high sensitive gamma-ray spectrometer with detector volume of 50,000 cc of NaI (TI). The data recorded in four channels were measured in the following energy window: Total counts 0.40-3.00 MeV; Potassium (^{40}K) 1.36-1.56 MeV; Uranium (^{214}Bi) 1.66-1.86 MeV; and Thorium (^{208}Tl) 2.42-2.82 MeV (Minty 1997, Fortin, et. al.2017) Fig.2.

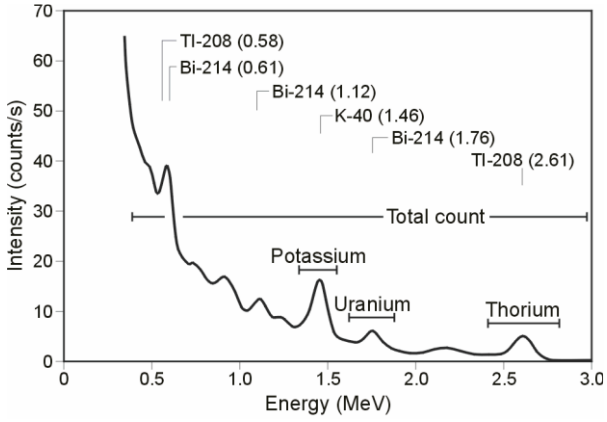

Figure 2: Gamma-ray spectrum showing three standard photopeak's and windows for Total counts, K, U and Th, and other photo peaks from the decay chain of U, Th and K.

The data were collected every second at the flying height of 120 meters above ground level with 1 km line spacing. The twin engine aircraft (Dakota DC-3) was visually navigated. and was supported by Inertial Navigation System. Pre-processing of AGRS data were carried out at Computer Centre of Atomic Minerals Directorate. Pre-processing includes cosmic and atmospheric background correction, height correction, inter-channel correction, and determination of system sensitivity the detailed account of the data acquisition and preprocessing is described elsewhere by Hovgaard and Grasty 1997, Dhurandhar and Saxena 1999.

3. Processing Methods

The pre-processed AGRS data of Komanutola area (10 lines-lat. 14° 19' - 14° 35'; Long. 74° 00'-74° 05') and Giddankipalle area (20 lines) - Lat. 14° 05' - 14° 35'N; Long 78° 15' - 78° 26'E) was taken up for present study. The counts per second data were converted into ppm for uranium, thorium and percentage for potassium. flight line stack profiles were generated for total cps, eU eTh (ppm), K (%) and their ratios eU/eTh, eU/K and eTh/K. the stack profiles were correlated with the Landsat image interpreted map of the area and excellent correlation of lithology with AGRS data was found (Dhurandhar et. al. 1991). After defining the lithological formations for each flight line, stack profile of the AGRS data belonging to specific lithological formations of Komanutola block were classified. percentile estimation is done for determination of NGF and AGF for each rock type i.e. Peninsular gneiss. Closepet granite, Gulcheru Formation, Lower and Upper Vempalle Formations, and Pulivendla Formation (Fig.3). The median (p50 = 50% of cumulative frequency) is used instead of arithmetic mean because the average represented by median is independent of the type of distribution of the parameter whereas arithmetic mean varies considerably with the type of distribution. When median (Me) is used standard deviation (σ) is determined by quartiles (Yufa and Gurvich 1964):

$$\sigma = \tfrac{3}{4} (Q_3 - Q_l) \quad (1)$$

Upper and lower limits of NGF are determined by using formula given by Yufa and Gurvich 1964:

$$NFu = Me + 1.5 (Q_3 - Me) \quad (2)$$

$$NFl = Me - 1.5 (Me - Q_l) \quad (3)$$

where Ql and Q3 are 25% and 75% of cumulative frequencies respectively. Lower limit of AGF is determined at 2σ above the median (Table 2).

4. Geological Setting

The Proterozoic Cuddapah basin is arcuate convex to the west the present study area lies in the southern convex part (Fig. 3). The Archaean crystalline which form the basement for Cuddapah Supracrustals are composed of Peninsular Gneiss and Clospet granite which is intrusive into the Peninsular Gneiss and crops out as inselbergs. The dolerite dyke swarms form Formation comprising conglomerates and quartzites shows cuesta-hogback landforms followed by shales, dolomite and stromatolytic limestones of lower Vempalle Formation which forms karst topography. The upper Vempalle Formation comprises shaly and stromatolytic limestones, which occasionally form cuesta-hogback landform. This is followed. by hard and indurated conglomerate quartzites of Pulivendla Formation which is overlain by Tadpatri shales; towards the top of

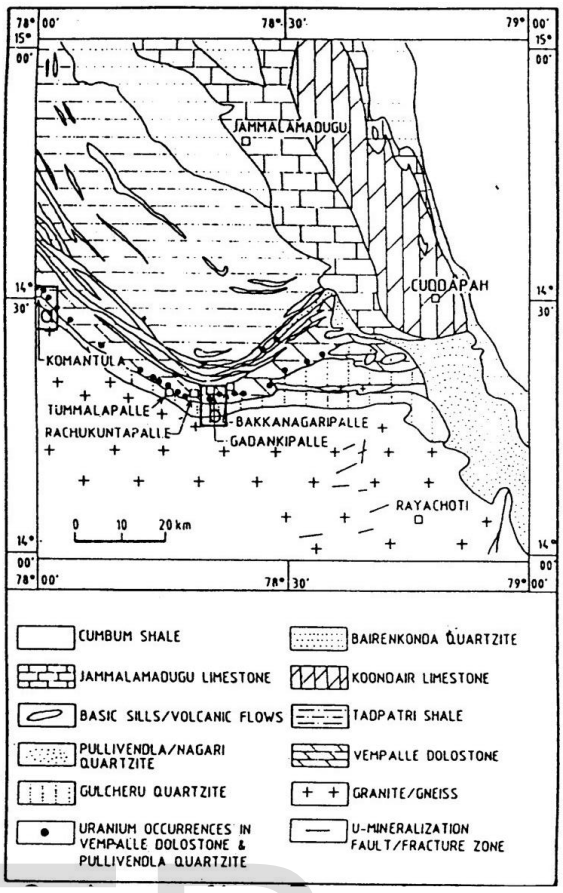

Figure 3. Geological map of the southern Cuddapah Basin after Rao et. al. 1989.

Vempalle Formation signs of volcanism are seen with sills and dolerite intrusions. The generalized stratigraphic succession of the study area (Nagaraja Rao, et. al. 1987) is given in Table 1. The lower Vempalle phosphatic dolomite hosts a number of uranium occurrences (Rao et al. 1989). Since the sedimentary sequence has large variation in rock chemistry, physical properties, sparse vegetation and thin soil cover, characteristic gamma-ray spectral signature is observed and integrated with geology and satellite image and SRTM digital elevation model Fig. 4b and 4c (Dhurandhar and Kumar, 1990, Dhurandhar 2018).

5. Lithological Interpretations

Total cps, eU and eTh in ppm, and K % flight line stack profile data classified into lithological type (Galbraith and Saunders 1983) and computerized geologic analysis of radiometric data are done as per the methodology given by Potts 1976. The main formation studied in detail are as follows:

5.1. Peninsular Gniess

Peninsular Gneisses are classified as granodiorite, tonalite and trondhjemite (Radhakrishna, 1990) at places they are migmatitic. Some trends of the relicts of Kadri schist belts are also present at few places. The transported soil covers the relict Kadri schist belt hence was not differentiated in AGRS data. Dolerite dykes intruded into

Figure 4a: Landsat Image showing the blocks under present study and Uranium occurences.

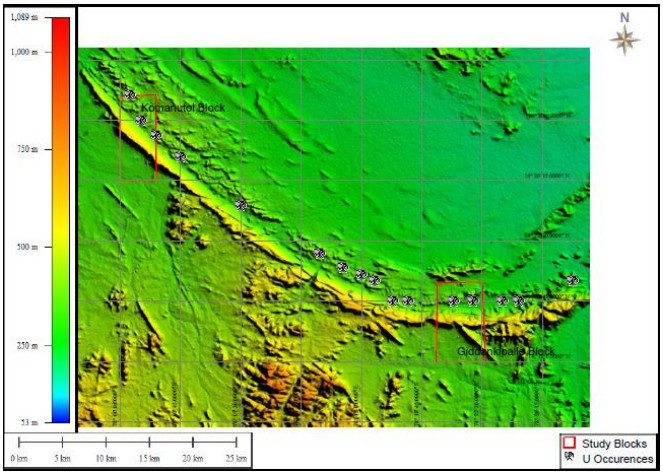

Figure 4b: SRTM Image showing the blocks under present study and Uranium occurences.

peninsular gneisses are represented as sharp drop of flattened stack profile. The median value of eU, eTh and K are comparable with the crustal abundances of the radioelement in granodiorite. The NGF for this rock type is total cps 974 to 2366, eU 1.3 to 2.9 ppm, eTh 2.8-12.3 ppm and K 0.7-1.9% (Figure 5; Table 2).

5.2. Closepet Granite

Clospet granite is considered as intrusive younger acidic granite (Radhakrishna, 1990) and are present in the form of highly fractured inselbergs. The median value of eU and eTh concentrations are higher than the crustal abundances of radioelement in the similar rocks and K concentration is comparable with the same. The NGF for closepet granite is 2824-7006 total cps,2.7-8.4 ppm eU, 29.8-51.5 ppm eTh, and 1.9-3.5% K. These rocks are characterized by highest radioactivity in the study area (Figure 5; Table 2). The radioactive anomalies are mainly due to high K content. eU and eU/eTh show very NGF whereas eU/K has very small value therefore, anomaly hasn't been picked in this rock type.

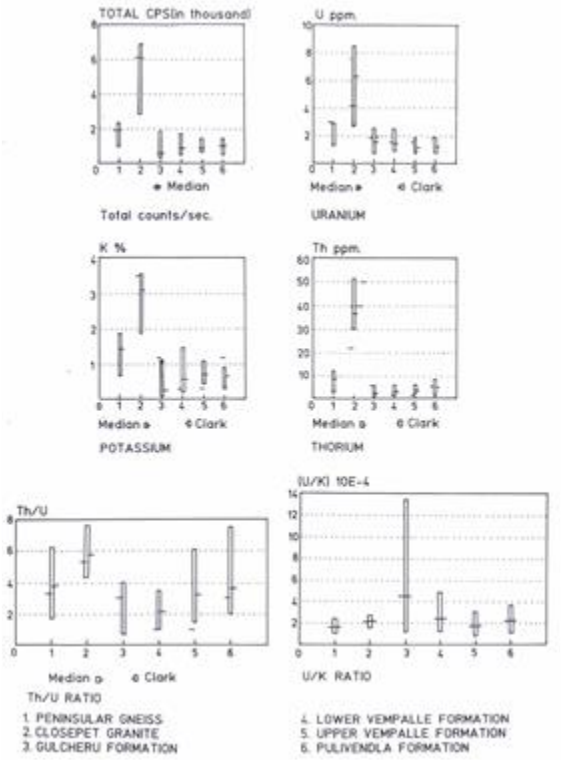

Figure 5: Normal Geochemical Fields in various formations of Cuddapah Basin and adjoining rocks.

5.3. Gulcheru Formation

This is the oldest formation in Cuddapah Supergroup and unconformably overlies the Peninsular Gneiss, comprising basal polymictic conglomerate followed by arkosic quartzite. The radioelemental concentrations in this formation is lower than the crustal abundances in sandstone /quartzite (Table 3). The NGF for total counts is 388-1875 cps, eU 0.7-2.5 ppm, eTh 1-5.8 ppm and K 0.1-1.1% (Figure 5, Table 2). Ratios eU/eTh and eU/K show larger NGF but inherent eU has considerably smaller NGF, thereby indicating lesser probability of finding any anomaly.

5.4. Vempalle Formation

5.4.1. Lower Vempalle Formation

The lower vempalle formation comprises of phosphatic dolomite, thin layer of purple shale and stromatolytic limestone. These were deposited in carbonate tidal flat environment (Nagaraja Rao et. al. 1987). The radioelemental concentration is typically higher than the crustal mean of eU, eTh, and K in carbonate rocks (Table 3). The NGF for total counts is 460-1665 cps, eU 0.9-2.6 ppm, eTh 1.6-5.9 ppm, and K 0.2-1.5%. The larger NGF for eU, eTh, K and eTh/eU indicate the anomalous nature of the formation (Fig. 5, Table 2).

5.4.2. Upper Vempalle Formation

This unit conformably overlies the Lower Vempalle Formation and comprises of stromatolytic limestone. The characteristic NGF for this unit (Figure 2) is 658-1428 total cps, eU 0.8-1.8 ppm, eTh 2.3-6.1 ppm and K 0.4-1.1%. The eU content (1.2 ppm) is less than the crustal mean of carbonate rocks (1.6 ppm) whereas potassium and thorium are higher than the crustal mean. The presence of impurities in limestone (chemogenic sediments) is responsible for higher eTh concentration (Table 3) and the impurities increase with the increase in stromatolite density in Upper Vempalle limestone.

Table 3: Comparison of Clark values with airborne gamma-ray spectrometric data

Rock types/Formations	Values	eTh (ppm)	eU (ppm)	K (%)
Intermediate (Granodiorite)	Clark	9.8	3	2.4
Peninsular Gneiss	AGRS	7.9	2.1	1.3
Acidic Granite	Clark	21.9	4.1	3.5
Closepet Granite	AGRS	28.2	5.9	2.8
Sandstone	Clark	5.7	1.9	1.2
Gulcheru Formation	AGRS	4	1.8	0.61
Pulivendla Formation	AGRS	5.5	1.3	0.63
Carbonate	Clark	1.6	1.6	0.3
Lower Vempalle Formation	AGRS	3.7	1.8	0.8
Upper Vempalle Formation	AGRS	4.1	1.3	0.8

Source: Clark values by Rogers, JJ.W., and Adams, JAS., (1969 a and b), In: Handbook of Geochemistry K. H. Wedepohl (Editor).

5.5. Pulivendala Formation

This forms the lowermost horizon of Chitravati Group and unconformably overlies Upper Vempalle Formation. Pulivendla Formation comprises polymictic conglomerate at the base and is overlained by arkosic quartzite. The NGF for this formation is total counts 515-1405 cps, eU 0.8-1.9 ppm, eTh 1.9-8.8 ppm, and K 0.3-0.9%. The median values of radioelements are comparable to the. crustal mean in sandstone. Only the K content 0.7% is much less than the crustal mean 1.2% (Figure 5, Table 2).

5.6. Geochemical Interpretation

The total radioactivity can be used to distinguish rock types but it cannot be used for identifying rock types. Various combinations of eU, eTh, and K may yield the same total radioactivity. Total radioactivity can detect areas of anomalous radioactivity but it cannot reveal the nature of anomaly (Schwarzer and Adams, 1973). The eTh and K concentrations can be used for rock discrimination. However, from the mineral exploration and metallogenic view-point ratios have more significance than absolute abundance (Darnley and Grasty, 1971). Particularly eTh/eU ratio varies with sedimentary facies and indicates uranium depletion. or accretion as well. The NGF for various formation (Figure 5) shows that the Peninsular Gneiss and Clospet granite have high eTh/eU ratios indicating uranium depletion. Gulcheru and Lower Vempalle Formations have low eTh/eU ratios suggesting possible host rocks for uranium mineralization. Upper Vempalle Formation has high eTh/eU ratio (Me=3.2), Pulivendla Formation has reworked sediments thereby characterized by high eTh/eU ratio because thorium has remained in detrital particles during the transport whereas uranium is leached out. eU/K ratio in Peninsular Gneiss and Clospet granite has lower NGF evidenced by high K concentration as compared to uranium. Only Gulcheru Formation shows higher NGF and higher median value indicating less potash content and less intrinsic uranium content. Therefore, no anomaly was located whereas lowerVempalle Formation has large NGF for eU/K and less

Table 2: Normal and Anomalous geochemical fields in various formations of Cuddapah Basin and adjoining rocks.

Formation / AGRS Parameters	Lower Quartile (Q1)	Upper Quartile (Q3)	Median (M)	Stadard Deviation (σ)	Normal Geochemical Field (NGF)		Anomalous Geochemical Field (AGF)	Coefficient of Variation
					Normal Field Lower	Normal Field Upper	Threshold	
Peninsular Gneiss (N=1377)								
Total Cps	1281	2209	1896	696	974	2366	3288	0.37
Uppm	1.5	2.6	2	0.8	1.3	2.9	3.7	0.41
K%	0.9	1.8	1.4	0.6	0.7	1.9	2.7	0.42
Th ppm	4.7	11	8.5	4.8	2.8	12.3	18	0.56
$U/Kx10^{-4}$	1.2	2.1	1.6	0.7	1	2.4	3	0.45
$(Th/Kx\ 10^{-4}$	5	7.4	6.2	1.8	4.4	0.8	9.7	0.29
Th/U	2.4	5.4	3.8	2.3	1.7	6.2	8.3	0.59
Closepet Granite(n=557)								
Total Cps	3913	6701	6091	2091	2824	7006	10273	0.34
Uppm	3.9	7.7	6.3	2.9	2.7	8.4	12	0.45
K%	2.3	3.4	3.1	0.8	1.9	3.5	4.8	0.27
Th ppm	32.2	46.7	36.8	10.9	29.8	51.6	58.6	0.3
$U/Kx10^{-4}$	1.7	2.6	2.2	0.6	1.5	2.7	3.4	0.28

Formation / AGRS Parameters	Lower Quartile (Q1)	Upper Quartile (Q3)	Median (M)	Stadard Deviation (σ)	Normal Geochemical Field (NGF)		Anomalous Geochemical Field (AGF)	Coefficient of Variation
					Normal Field Lower	Normal Field Upper	Threshold	
Th/U	4.7	7	5.7	1.7	4.3	7.6	9.1	0.29
Gulcheru Fm. (N=389)								
Total Cps	457	1448	595	749	388	1875	2082	1.25
Uppm	1	2.2	1.6	0.9	0.7	2.5	3.4	0.56
K%	0.1	0.8	0.3	0.5	0.1	1.1	1.3	2.09
Th ppm	1.5	4.7	2.5	2.4	1	5.8	7.3	0.95
U/Kx10^{-4}	2.3	10.5	4.5	6.2	1.2	13.5	16.9	1.38
(Th/Kx 10^{-4}	5.9	15	9.6	6.8	4.1	17.7	23.2	0.71
Th/U	1.1	3.3	2	1.7	0.7	4	5.3	0.83
Lower Vempalle Fm. (N=550)								
Total Cps	592	1396	586	603	460	1666	2062	0.7
Uppm	1.1	2.2	1.5	0.8	0.9	2.6	3.2	0.55
K%	0.3	1.2	0.6	0.6	0.2	1.5	1.8	1.13
Th ppm	2.2	5	3.3	2.1	1.6	5.8	7.6	0.64
U/Kx10^{-4}	1.6	4.1	2.5	1.9	1.2	4.9	6.2	0.75
(Th/Kx 10^{-4}	3.7	7.8	5.2	3.1	3	9.1	11.3	0.59
Th/U	1.4	3.1	2.1	1.3	1	3.5	4.7	0.6
Upper Vempalle Fm.(N=557)								
Total Cps	736	1249	892	385	658	1428	1662	0.43
Uppm	0.9	1.6	1.2	0.5	0.8	1.8	2.3	0.44
K%	0.5	1	0.7	0.3	0.4	1.1	1.3	0.47
Th ppm	2.8	5.3	3.8	1.9	2.3	6.1	7.6	0.49
U/Kx10^{-4}	1.1	2.6	1.7	1.2	0.8	3.1	4	0.66
(Th/Kx 10^{-4}	3.7	8.1	5.6	3.3	2.7	9.4	12.2	0.6
Th/U	2	5.1	3.2	2.3	1.4	6.1	7.8	0.72
Pulivendla Fm. (N=88)								
Total Cps	677	1271	1004	445	515	1405	1894	0.44
Uppm	1	1.7	1.3	0.6	0.8	1.9	2.4	0.43
K%	0.4	0.8	0.7	0.3	0.3	0.9	1.3	0.48
Th ppm	3	7.6	5.2	3.4	1.9	0.8	12	0.67
U/Kx10^{-4}	1.5	3.2	2.2	1.3	1.1	3.7	4.9	0.59
(Th/Kx 10^{-4}	6.7	10.9	0.5	3.2	5.8	12.1	14.9	0.37
Th/U	2.5	6.2	3.6	2.8	1.9	7.5	9.2	0.76
Note: N=AGRS data/sec.								

for eTh/eU and higher eU content (Me=2.1 ppm) as compared to carbonate rocks. Therefore, evidenced by number of anomalies whereas in comparison to this Upper Vempalle Formation has smaller NGF for eU/K. The same is found correct for Pulivendla quartzite as compared to Gulcheru quartzite (Fig. 5, Table 2).

6. Uranium Favourability Index

On the basis of known source and host rocks in Wyoming Dodd (1976) proposed coefficient of variation as uranium favourability index (UFI) (Pircle et. al. 1982). The higher index value is indicative of high potentiality for anomalously low or high uranium concentration. By using this approach no conclusive interpretation can be done. Subsequently, Saunders (1979) proposed three indices designated UI, U2, and U3 based on aerial radiometric data from Alaska. Ul, U2, and U3 are computed to give increasing index values with increasing uranium favourability in sandstone. These indices are defined as follows:

$$U1 = \frac{(MeU + MeTh + MK).RSD(eU).RSD\left(\frac{eU}{eTh}\right).RSD\left(\frac{eU}{K}\right)}{M\left(\frac{eU}{eTh}\right).M(eU/K)} \quad 4$$

$$U2 = \frac{MeU}{\left(\frac{MeU}{eTh}\right).\left(\frac{MeU}{MK}\right)} = \frac{MeTh.MK}{MeU} \quad 5$$

$$U3 = \frac{1}{\left(\frac{MeU}{MeTh}\right).\left(\frac{MeU}{MK}\right)} = \frac{MeTh.MK}{MeU} \quad 6$$

Where, M is the median quadrangle value and RSD, the relative standard deviation (σ/μ). All parameters which increase with the increasing uranium potentials are in the numerator and the denominator decreases with the increasing uranium potential. We believe that the quadrangle median used by Saunders is a poor approximation, where many lithologies are present in a quadrangle, the same applies for RSD also. It is, therefore, we looked for an alternative the observations made for phosphatic dolomite of Lower Vempalle Formation show that the eTh and K are very low. Therefore, eU/eTh and eU/K increase with increasing uranium potential and the following equation was derived which is inverse of Saunders' equation (5):

$$UFI = \frac{\left(\frac{eU}{eTh}\right).\left(\frac{eU}{K}\right)}{eU} = \frac{eU}{eTh.K} \quad 7$$

Where eU and eTh are in ppm and K in percentage.

The UFI profiles were generated for each flight line for both Komanutola and Giddankipalle areas. The UFI values were then gridded and contour map was generated using inverse square distance method. The UFI map gives precise location

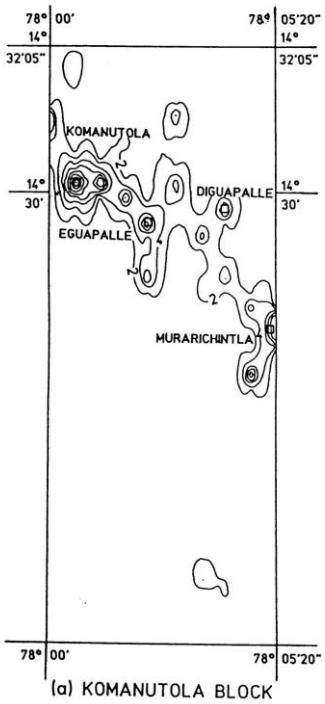

Figure 6a: Uranium favourability Index map of Komanutola block.

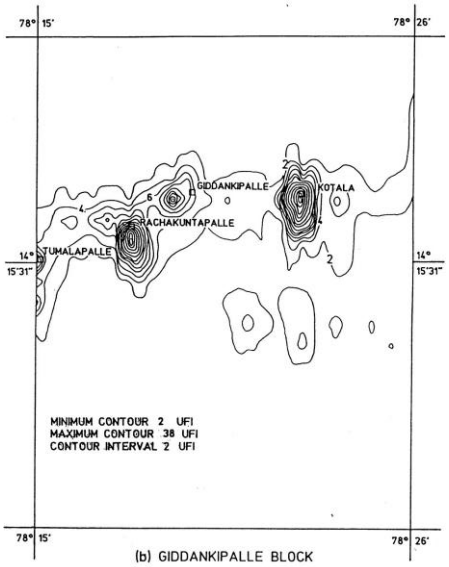

Figure 6b: Uranium favourability Index map of Giddankipalle block

and trend of uranium anomalies (Figure 6a and b) in phosphatic dolomite. The UFI values of various anomalies are shown in Table 4. Though the correlation between UFI values and the grade is approximate but. high UFI values have helped in delineating the areas of uranium mineralization. Determination of UFI is a complex procedure and requires knowledge of geochemistry of the lithology in terms of eU, eTh and K. The UFI is rock specific and may or may not be applicable for other rock types.

Table 4: Uranium Favourability Index and the physical assay values of some anomalous areas.

Area	Uranium favourability Index (UFI)	Physical Assay % eU_3O_8
Komanutola	21	0.02
Diguapalle	10	0.01
Eguapalle	12	0.01
Tummalpalle	38	0.04
Rachkuntapalle	38	0.03
Giddankipalle	30	0.04

7. Conclusions

The present work suggests that the profile data analysis for geological and geochemical interpretations is better than the analogue (contour) maps where due to gridding and interpolation of data minor variations in lithology are not identifiable, particularly those features which occur at an acute angle to the flight line. Geological classification of broad lithological formations can be done using NGF. The geochemical studies for various Formations are essential for deriving uranium favourability index. The conventional data integration by using contour maps of eU, eU/eTh and eU/K has not help in targeting all the anomalies whereas the proposed UFI mapping has helped to delineate high as well as low order anomalies very effectively. Thus, the present studies have established the utility of the geochemical analysis for mapping uranium favourable areas within thematic geological settings

8. Acknowledgements

Author is grateful to The Atomic Minerals Directorate for Exploration and Research for all the logistics and computing facilities to carry out the work. I am thankful to the crew members associated with the AGRS data acquisition, preprocessing and Physics Laboratory for sample analysis. Author is also thankfull to anonymous reviewer for his comments to improve the quality of paper.

References

[1] Armstrong, F.E., and R.J. Heemstra, 1973: Radiation halos and hydrocarbon reservoirs, a review. US Bureau of Mines, Information Circular 8579.

[2] Busby, J. P. Peart, R. J. Green, C. A. Ogilvy, R. D. and Williamson, J. P. (1991). A search for direct hydrocarbon indicators in the Formby area. Geophysical Prospecting, v. 39, pp. 691-710.

[3] Darnley, A. G., and Fleet, M. (1968). Evaluation of airborne gamma ray spectrometry in the Bancroft and Elliot lake areas of Ontario, Canada, Proc. Fifth Symposium on remote sensing of environment, Ann Arbor, Univ. Michigan, p. 833-853.

[4] Darnley, A. G., (1970). Airborne gamma ray spectrometry, Canadian Inst. Mining Metallurgy Trans. v. 3, p.20-29.

[5] Darnley, A. G., (1971). Aeroaradiometric survey techniques: NATO Adv. study Inst. methods prospecting uranium minerals, London, Sept. 21 - Oct. 2, p. 1-27.

[6] Darnley, A. G. and Grasty, R. L, (1971). Mapping from the air by gamma-ray spectrometry: Proc. Third Internatl. Geochem. Explor. Symposium, Toronto, ClM., spec. v.11, p. 485-500.

[7] Darnley, A. G., (1973). Airborne gamma-ray survey technique- Present and Future, Uranium Exploration Methods, Proc. series International Atomic Energy (IAEA) Vienna, p: 67-108.

[8] Dhurandhar, A. P. and Kumar, C. S. (1990). Geological analysis of remotely sensed data and integration with airborne gamma-ray spectrometric data of Dhone-Jakkasanikuntla area (AP.), Unpub. Rept. At. Minerals Dir., Hyderabad.

[9] Dhurandhar, A. P., Katti V. J, and Dattanarayana, T. A (1991). Geochemical analysis of airborne gamma-ray spectrometric data, parts of Cuddapah basin, (A.P.), Unpub. Rept. At. Minerals Dir. Hyderabad.

[10] Dhurandhar A. P. and Saxena D.N. (1999): Integrated airborne gamma ray spectral and satellite data analysis for U and REE mineralization - A case study from north Sagobandh area, District Sonbhadra, Uttar Pradesh, India. Indian Soc. Remote Sensing v. 27, No.1, pp 43-57.

[11] Dhurandhar A. P. (2018): Integration of Satellite data and SRTM digital elevation model for lithostructural mapping, Unpub. Rept. Orion Geohytech, Nagpur.

[12] Dodd, P. M., (1976). Airborne radiometric reconnaissance: The why's and where-fore's: Uranium geophysical technical symposium summaries and visual presentations, U S. Energy Res. Dev. A demand, Bendix Field Engineering Corpn. Grand Junction Colorado, Sept. 14-16, p. 13-20.

[13] Fortin, R., Hovgaard, J., Bates, M. (2017). Airborne Gamma-Ray Spectrometry in 2017: Solid Ground for New Development. In "Proceedings of Exploration 17: Sixth Decennial International Conference on Mineral Exploration" edited by V. Tschirhart and M.D. Thomas, 2017, p. 129–138

[14] Frederic L. Pircle, Richard, J. Beckman, and H. L. Fleischhaur Jr., (1982). Multivariate uranium favourability index using aerial radiometric data, Jour. Geol. v.90, p. 109-124.

[15] Galbraith, H. J., and Saunders, D. F., (1983). Rock classification by characteristics of aerial gamma-ray measurements, Jour. Geochem. Explor. v. 18, p. 49-73.

[16] Grasty, R.L. and B.R.S. Minty, (1995): A guide to the technical specifications for airborne gamma ray surveys: Australian Geological Survey Organization Record 1995/60.

[17] Hovgaard, J. and Grasty, R.L. (1997). Reducing Statistical Noise in Airborne Gamma-Ray Data through Spectral Component Analysis. In "Proceedings of Exploration 97: Fourth Decennial International Conference on Mineral Exploration" edited by A.G. Gubins, 1997, p. 753–764

[18] IAEA, (1991): Airborne Gamma Ray Spectrometer Surveying: International Atomic Energy Agency, Vienna, Tecdoc-323.

[19] IAEA, (2003): Guidelines for radioelement mapping using gamma ray spectrometry data: International Atomic Energy Agency, Vienna, Tecdoc-1363.

[20] Katti V. J. Dattanarayana, T. A Shrihari, R. and Kak, S. N. (1997): Radiation monitoring in the environs of nuclear power plants in India using airborne gamma ray spectrometry. Exploration and Research for Atomic Minerals, v. 10 p. 107-118.

[21] Minty B.S.R. (1997). Fundamentals of Airborne Gamma Ray Spectrometry, Jour. Australian geology and geophysics 17 (2) p.39-50

[22] Mohamed A. S. Youssef and Shadia T. Elkhodary (2013). Utilization of airborne gamma ray spectrometric data for geological mapping, radioactive mineral exploration and environmental monitoring of southeastern Aswan city, South Eastern Desert, Egypt, *Geophys. J. Int.* (2013) 195, 1689–1700

[23] Nagaraja, Rao B. K., Rajurkar, S. T., Ramlingaswami, G., and Ravindra Babu, B., (1987) Stratigraphy, structure and evolution of the Cuddapah basin, Purana Basins of Peninsular India, Radhakrishna, B.P. (Editor) B. B. D., Bangalore, p. 33-896.

[24] Neuschel, S. K., (1970). Correlation of aeromagnetics and aeroradioactivity with lithology in Spotsylvania area Virginia, Geol. Soc. America Bull., v. 12, p. 3575-3582.

[25] Neuschel, S. K., (1971). Correlation of uranium, thorium and potassium with aeroradioactivity in Berar area Virginia, Econ. Geol. v. 66, p. 302-308.

[26] Pitkin, J. A, (1968). Airborne measurements of terrestrial radioactivity as an aid to geologic mapping, United State Geological Survey (USGS) Prof paper 5l6-F, p. Fl-F29.

[27] Potts, M. J., (1976). Computer methods for geologic analysis of radiometric data, In: Exploration for uranium ore deposits, Proc. Series, IAEA SM 208/46, International Atomic Energy Agency (IAEA), Vienna, p. 55-69.

[28] Radhakrishna, B. P., (1990). Archaean granite-greenstone terrain of the south Indian shield, In:

Archaean greenstone belts of south India, Radhakrishna B. P. and Ramakrishna M. (Editors) B. B. D. Bangalore, p. 180-221.

[29] Rogers, J. J. W. and Adams, J. AS., (1969) a. Uranium, In: K H. Wedephol (Editor) Handbook of Geochemistry, v. *II/1*, Springer-Verlog, Berlin, Chapter 92.

[30] Rogers, J. J. W. and Adams, J. AS., (1969) b. Thorium, In: K H. Wedephol Editor) Handbook of Geochemistry, v. *II/1*, Springer - Verlog, Berlin, Chapter 90.

[31] Rao, M. V. Nagbhushana,1. C. and Jeygopal, A V. 1989). Uranium mineralization in the middle Proterozoic carbonate rock of the Cuddapah Supergroup, Southern Peninsular India. Explor. Res. Atomic Minerals v.2, pp29-38.

[32] Saunders, D. F., (1979). Characterization of uraniferous geochemical provinces by aerial gamma-ray spectrometry, Mining Engineering December, p. 1715-1722.

[33] Schwarzer, T. F., Cook, B. G., and Adams, J. AS., (1972). Low altitude gamma-ray spectrometric surveys from helicopters in Puerto Rico as an example of the remote sensing of thorium, uranium and potassium in rocks and soils, Remote Sensing Environment, v.2, p. 83-94.

[34] Schwarzer, T. F., and Adams, J. A.S., (1973). Rock and soil discrimination by low altitude airborne gamma-ray spectrometry in Payne County, Oklahoma, Econ. Geol. v. 68, p. 1297-1312.

[35] Shuttle Radar Topography Mission (SRTM) Technical Guide: Global Land Cover Facility, University of Maryland Institute for Advanced Computer Studies, University of Maryland Department of Geography. Primary Links for SRTM Project: http://www2.jpl.nasa.gov/srtm/ ; http://srtm.usgs.gov/; http://landsat.gsfc.nasa.gov/documentation/wrs.html;

[36] Sikka, D. B., and R. B. K. Shives, (2002). Radiometric surveys of the Redwater oil field, Alberta: Early surface exploration case histories suggest mechanisms for the development of hydrocarbon-related geochemical anomalies. In D. Schumacher and L. A. LeSchack, eds., Surface exploration case histories: Applications of geochemistry, magnetics, and remote sensing, AAPG Studies in Geology No. 48 and SEG Geophysical References Series No. 11, p. 243–297

[37] Yufa, B. Ya., and Gurvich, Yu. M., (1964). The use of the median and quartiles in estimating normal and anomalous values of a geochemical field, Geochem. Int. No.4, p. 801-806.

Author Profile

Ashokaditya P. Dhurandhar received the B.Sc. degree in 1984 from A. P. S. University Rewa, M.Tech. degree in Applied Geology from National Institute of Technology Raipur (NITRR), India in 1987, MBA in Systems from Sikkim Manipal University, Gangtok, India in 2009. During 1988-2010, he stayed in Atomic Minerals Directorate for Exploration & Research Department of Atomic Energy Government of India. He has Certifications on Remote Sensing, Spectral Remote Sensing, GIS from Indian Institute of Remote Sensing, Dheradun and UNESCO, Geophysical, Geochemical Exploration, Reserve, Resource Estimation, Mining, and Mine Planning, from Atomic Minerals Directorate (AMD), Indian Bureau of Mines (IBM) and CRIRSCO, Strategic Management from National Institute of Industrial Engineering (NITIE) Mumbai India. Later on, from 2010 onwards he is leading research projects for Exploration, mining and plant erection and commissioning for several minreals, metals, Oils and Gas in severals listed and unlisted companies in several countries across the globe viz. Asia, Africa, America and Europe. He is a Professional Geologist, Hydrogeologist, Geotechnical Engineer and Competent Person for Major, Minor, Radioactive, Strategic minerals, metals and prescribed substances. His special expertise lies in Exploration of Radioactive Minerals, Precious metals, strategic metals and minerals.